Variation in flexural properties of photo-pultruded composite archwires: analyses of round and rectangular profiles

D. W. FALLIS[1], R. P. KUSY[1,2,3]*
[1]Department of Orthodontics, [2]Department of Biomedical Engineering, [3]Curriculum in Applied and Material Sciences, University of North Carolina at Chapel Hill, Chapel Hill, NC 27599–7455, USA
Email: rkusy@bme.unc.edu

Prototype continuous, unidirectional, fiber-reinforced composite archwires were manufactured into round and rectangular profiles utilizing a photo-pultrusion process. Both 0.022 inch (0.56 mm) diameter and 0.021×0.028 inch (0.53×0.71 mm) rectangular composites were formed utilizing commercially available S2-glass® reinforcement within a polymeric matrix. Reinforcement was varied according to the number, denier and twists per inch (TPI) of four S2-glass® yarns to volume levels of 32–74% for round and 41–61% for rectangular profiles. Cross-sectional geometry was evaluated via light microscopy to determine loading characteristics; whereas two flexural properties (the elastic moduli and flexural strengths) were determined by 3-point bending tests. Morphological evaluation of samples revealed that as the TPI increased from 1 to 8, the yarns were more separated from one another and distributed more peripherally within a profile. For round and rectangular profiles utilizing 1 TPI fibers, moduli increased with fiber content approaching theoretical values. For round profiles utilizing 1 TPI and 4 TPI fibers, flexural strengths increased until the loading geometry was optimized. In contrast, the flexural strengths of composites that were pultruded with 8 TPI fibers were not improved at any loading level. Doubling the denier of the yarn, without altering the loading, increased both the moduli and flexural strengths in rectangular samples; whereas, the increases observed in round samples were not statistically significant. At optimal loading the maximum mean moduli and strengths equaled 53.6 ± 2.0 and 1.36 ± 0.17 GPa for round wire and equaled 45.7 ± 0.8 and 1.40 ± 0.05 GPa for rectangular wires, respectively. These moduli were midway between that of martensitic NiTi (33.4 GPa) and beta-titanium (72.4 GPa), and produced about one-quarter the force of a stainless steel wire per unit of activation. Values of strengths placed this composite material in the range of published values for beta-titanium wires (1.3–1.5 GPa).

1. Introduction

Since the first patent issued for pultrusion in 1951, substantial advancements have been made in this industry [1]. Although the first market for this process was in the field of sporting goods (solid fiber-glass fishing rods), once techniques improved new markets soon opened up in the hardware, automotive, electronic, aerospace and medical fields [2]. In the past decade, several investigations have been conducted documenting the feasibility of thermally pultruded continuous fiber-reinforced composites in dentistry [3–7]. Recently, a novel approach for pultruding small diameter composites was designed utilizing photo-polymerization rather than heat-activated polymerization [8, 9] which has many advantages over conventional thermal pultrusion. These advantages include a solvent-free process, high-energy efficiency, and control of the initiation reaction [10].

The photo-pultrusion process has spawned interest into the development of small diameter, fiber-reinforced plastics for the orthodontic field. To determine clinical feasibility, *in vitro* investigations have characterized the steady-state sorption [11] and hydrolytic stability [12]. Highly reinforced composite profiles have been fabricated, having diameters of approximately 0.5 mm, that have demonstrated excellent flexural properties [13]. In addition, although rectangular materials have been fabricated utilizing a two-stage technique (beta staging) [14], to date only round profiles have been fabricated utilizing this continuous process.

With the vast number of orthodontic wires on the

*Author to whom correspondence should be sent.

market already demonstrating an array of flexural properties, aesthetics would appear to be the main advantage of these composites for tooth movement and tooth retention. However, more important structural advantages exist. Because the geometry of the reinforcement fibers can be altered internally, the overall dimensional profile can be maintained while the flexural modulus is varied to suit the individual treatment objectives. This remains a distinct advantage in the practice of variable modulus orthodontics where, for the same size and shape of wire, the alloy type is altered to achieve the flexural properties necessary to efficiently move teeth [15]. Since the composite's size, shape and chemistry are constant, more consistent wire-bracket couple interactions are possible. By maintaining more consistent wire-slot angular relationships, more reproducible levels of friction are achieved [16].

This investigation evaluates composites of round and rectangular, unidirectional, fiber-reinforced plastic (UFRP) profiles that were fabricated continuously using this novel photo-pultrusion process [8]. The bending tests demonstrate the influence of fiber-reinforcement parameters on elastic moduli and flexural strengths. These findings show that, at selected loading levels, moduli can be varied by incorporating twist within the reinforcing fibers without a reduction in flexural strength; likewise, increasing the denier of the reinforcement yarn can enhance flexural properties.

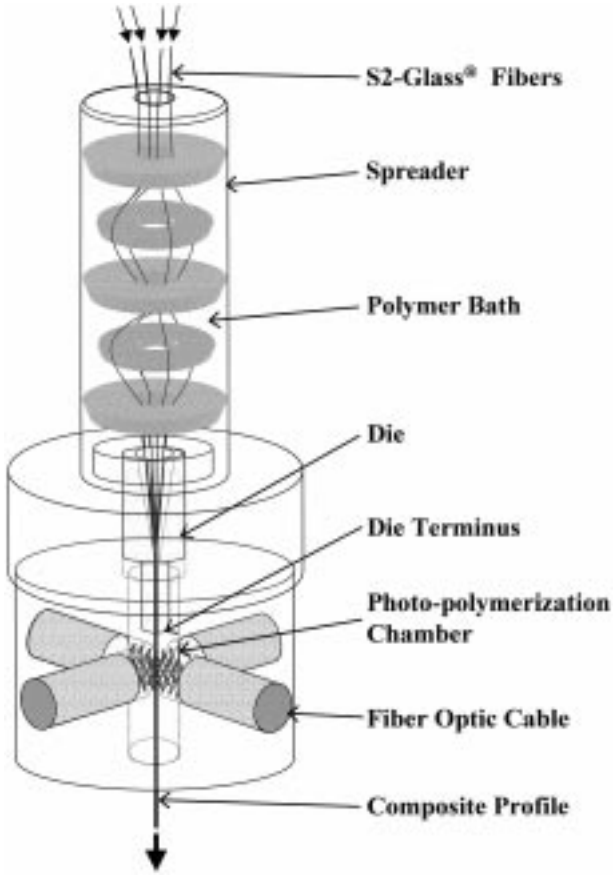

Figure 1 Schematic diagram of the photo-pultrusion apparatus showing fibers initially entering the spreader and the composite profile finally exiting the photo-polymerization chamber [8].

2. Materials and methods

2.1. Die fabrication

Round and rectangular forming dies were fabricated from a type 400 stainless steel, housed within an aluminum core, and inserted into the pultrusion apparatus (Fig. 1). The internal aspects of these dies were polished with a sequence of aqueous dispersions of Al_2O_3 (1.0–0.3 μm).

2.2. Material processing

Materials consisted of S2-glass® (magnesium aluminosilicate) fiber reinforcement (Owens-Corning Corp., Toledo, OH, USA) in a polymer matrix consisting of 61 %wt bisphenol-A diglycidyl-methacrylate (Bis-GMA, Nupol 046–4005, Cook Composites and Polymers Co., North Kansas City, MO, USA) and 39% wt triethyleneglycol-dimethacrylate (TEGDMA, Polysciences Inc., Warrington, PA, USA). Benzoin-ethyl-ether (Aldrich Chemical Co. Inc., Milwaukee, WI, USA), 0.4% wt was added for photo-initiation. The S2-glass® fibers were acquired in yarn form, which had been pre-sized with a proprietary organo-silane binder. Four glass yarn materials were chosen (Table I), which differed in denier[1] and TPI. These yarns are supplied with a denier equivalent of 300 (CG150) or 600 (CG75), with the 300 having 50% less bare glass yardage per pound. Since the filament diameter is held constant, this difference in denier results because of an increase in the number of filaments per yarn. All yarns had a counter-clockwise pre-twist in the ''Z'' direction. These and other important material product designations are annotated in the footnote of Table I.

Round and rectangular composite profiles were generated utilizing a previously documented photo-pultrusion process [8, 9] that incorporated a 300–450 nm UV-curing lamp with an output provided by a 100 watt mercury-vapor bulb (Lightwave Energy Systems Co. Inc., LESCO, Redondo Beach, CA). These materials were generated by a continuous process that varied the per cent loading of reinforcement every

TABLE I Specifications of S2 glass® yarns investigated

Material product designation*	Denier equivalent	Bare glass (yds/lb)	Filament diameter, d_f (μm)	Twists per inch (TPI)
S2 CG75 1/0 1.0Z 493	600	7 500	9	1
S2 CG150 1/0 1.0Z 493	300	14 900	9	1
S2 CG150 1/0 4.0Z 493	300	14 900	9	4
S2 CG150 1/0 8.0Z 493	300	14 900	9	8

*U.S. Customary System is used for fiberglass yarn nomenclature, where:
S2 denotes the type of glass yarn;
C denotes continuous fiber type;
G denotes filament diameter code of 9 microns;
75 denotes 1/100th the bare glass yardage per pound of strand, equal to 7500 yds/lb or 600 denier equivalent; or,
150 denotes 1/100th the bare glass yardage per pound of strand, equal to 15 000 yds/lb or 300 denier equivalent;
1/0 denotes 1 yarn without additional plies;
1.0Z denotes 1 twist per inch twisted in the ''Z'' direction (counter-clockwise); and
493 denotes the recommended sizing for use in Bisphenol-A type polymers.

300 cm. The per cent loading by volume of fiber ($\%V_f$) was varied in a nominal 0.022 inch (0.56 mm) round profile by staging the number of yarns incorporated into the pultrusion apparatus from three yarns ($32\%V_f$) to 14 yarns ($74\%V_f$). With the exception of S2 CG75 yarns, fabrication of composite materials with less than eight yarns resulted in the flow of resin past the yarns into the curing chamber, causing clumps of cured resin on the profile. Due to the larger size of the CG75 yarn, round profiles could be fabricated with only three yarns (equivalent to six CG150 yarns or $32\%V_f$). The loading in a nominal 0.021×0.028 inch (0.53×0.71mm), rectangular profile was varied in stages from 12 yarns ($41\%V_f$) to 18 yarns ($61\%V_f$). When a CG75 fiber was used, the number of yarns was halved.

2.3. Morphological examination

Samples were embedded in poly(methyl methacrylate), hand ground with SiC papers through 1200 grit and polished in a Buehler® Vibromet polisher (Buehler Ltd, Evanston, IL, USA) with a 1.0 μm Al_2O_3 aqueous dispersion. Gross morphological examination was conducted with a Zeiss universal reflected-light microscope (Carl Zeiss, Oberkochen, Germany).

2.4. Light source distance determination

Initial experimentation was conducted to produce and evaluate a material that was truly ''rectangular''. Because surface tension tends to cause the unpolymerized material to assume a round or oval profile, regardless of the die shape utilized, the optimal distance from the terminus of the die (Fig. 1) to the point of initial polymerizing light exposure was required. Profiles were polymerized at four points beginning 3 mm from the curing chamber and collected at each 1 mm increment of distance until the die terminus was in the chamber (0 mm from the light source).

Microscopic analysis revealed that the positioning of the die had profound effects on a profile's morphology. Positioning the die terminus at the maximum distance tested (3 mm from the curing chamber) resulted in surface-tension induced deformation; whereas, positioning at 0–1 mm from the chamber resulted in polymerization inside the forming die, causing partial blockage and poor geometry. The optimal geometry was achieved when the die terminus was positioned 2 mm from the entrance to the curing chamber. Since the rate of pultrusion was 1.27 mm/sec, this position placed the material within the curing chamber 1.6 s after exiting the die terminus.

2.5. Flexural properties

Utilizing 3-point bending in an Instron® Universal Testing Machine (Model TTCM, Instron Corp., Canton, MA, USA), five 20 mm long samples of each $\%V_f$ were tested at room temperature (23 °C). Diametral measurements of each sample were obtained utilizing a Sony μ-mate® Digital Micrometer (Sony Magnescale America Inc., Orange, CA, USA) by averaging the measurements made at five radial locations in the center of each sample.

Bending loads were applied to failure at a deflection rate of 0.1 cm/min. Values for elastic modulus (E) and flexural strength (FS) were calculated for each sample by utilizing Equations 1 and 2

$$E = PL^3/48I\delta \tag{1}$$

$$FS = Mc/I \tag{2}$$

where P = applied load, L = span length = 8.89 mm, I = area moment of inertia ($\pi D^4/64$ for round and $bh^3/12$ for rectangular profiles where D = diameter of sample, b = base of rectangle, and h = height of rectangle), δ = beam deflection, M = maximum bending moment and c = sectional dimension for round ($D/2$) and for rectangular ($h/2$) sections [18].

A fully-factorial multiple analysis of variance (MANOVA) was performed to determine significant differences in E and FS as a function of denier, the TPI, and $\%V_f$ (SYSTAT Version 5, SYSTAT Inc., Evanston, IL, USA). Statistical significance was ascribed to the results when a probability value of $p < 0.05$ was observed. P-values < 0.001 were noted as highly significant. Significant interactions were investigated further with the Tukey HSD post-hoc comparison of individual means.

2.6. Per cent loading determination

The $\%V_f$ of S2-glass® in each profile is dependent upon the overall dimensions and shape of the profile and the individual size, number, and TPI of each filament within the yarn. As the number of twists per inch of each yarn increases, the helix angle of each filament decreases. This has the effect of increasing the $\%V_f$ loading of S2 glass® in each profile due to the increased area of the ellipse formed by each filament in cross-section. Based upon the previously reported equation [19], the helix angle (α) for each filament can be calculated within the present context as

$$\alpha = \tan^{-1}[(\mathrm{TPI})(\pi)(d_y - d_f)]^{-1} \tag{3}$$

where d_y = overall diameter of a yarn [0.011 inch (0.28 mm) for CG75 and 0.008 inch (0.20 mm) for CG150], and d_f = component filament diameter (0.000354 inch $\approx$ 9 μm).

Once the helix angle is determined, the area (A) of the elliptical fibers can be calculated according to the equation

$$A = N\pi d_f d/4 \tag{4}$$

where N = number of filaments, d_f = length of the minor axis = component filament diameter, and d = length of the major axis = $d_f/\sin\alpha$.

Therefore,

$$A = N\pi d_f^2/4\sin\alpha \tag{5}$$

which for CG150 and CG75 yarns may be written as

$$A = 204\pi d_f^2/4\sin\alpha \tag{6}$$

and

$$A = 408\pi d_f^2/4\sin\alpha \tag{7}$$

respectively.

Finally, the $\%V_f$ may be obtained from A and the overall area of the round and rectangular composites may be written as

$$\%V_f = 100\mathrm{A}/(0.785\mathrm{D}^2) \quad (8)$$

and

$$\%V_f = 100\mathrm{A}/(\mathrm{bh}) \quad (9)$$

respectively.

3. Results

3.1. Morphological examination

The evaluation of round and rectangular profiles revealed that the loading characteristics and profile morphology changed when $\%V_f$ and/or TPI were altered (Figs 2–5). When loading and morphology in round profiles were evaluated at three different levels of $\%V_f$ and TPI, as the twist was increased from 1 to 8 TPI, increases in yarn isolation and intra-yarn voids are observed at each $\%V_f$ (Fig. 2). When the denier was doubled, the morphology of round profiles was altered (Fig. 3). When rectangular profiles were compared at six different levels of $\%V_f$, a marked improvement in the geometry was observed as the $\%V_f$ increased (Fig. 4). When rectangular profiles with a constant $\%V_f$ were compared at three different levels of TPI (Fig. 5), the same loading and morphological characteristics as those seen in round profiles were observed (Fig. 2).

3.2. Flexural properties

The $\%V_f$ determinations of round and rectangular profiles of differing TPI revealed that, as the twist increased from 1 TPI to 8 TPI, the $\%V_f$ of these small profiles never increased by more than 2% (Tables II and III). Therefore, nominal $\%V_f$s were used for all calculations, independent of TPI. The evaluation of round and rectangular profiles in 3-point bending revealed that altering $\%V_f$, denier, and TPI influenced Es and FSs (Figs 6 and 7). The mean values for the round and rectangular profiles were calculated and standard deviations (s.d.) determined (Tables II and III). Analysis of this data revealed that the variability of s.d.s among round profiles was generally below 15% of mean values for Es and FSs. The variability of s.d.s for rectangular

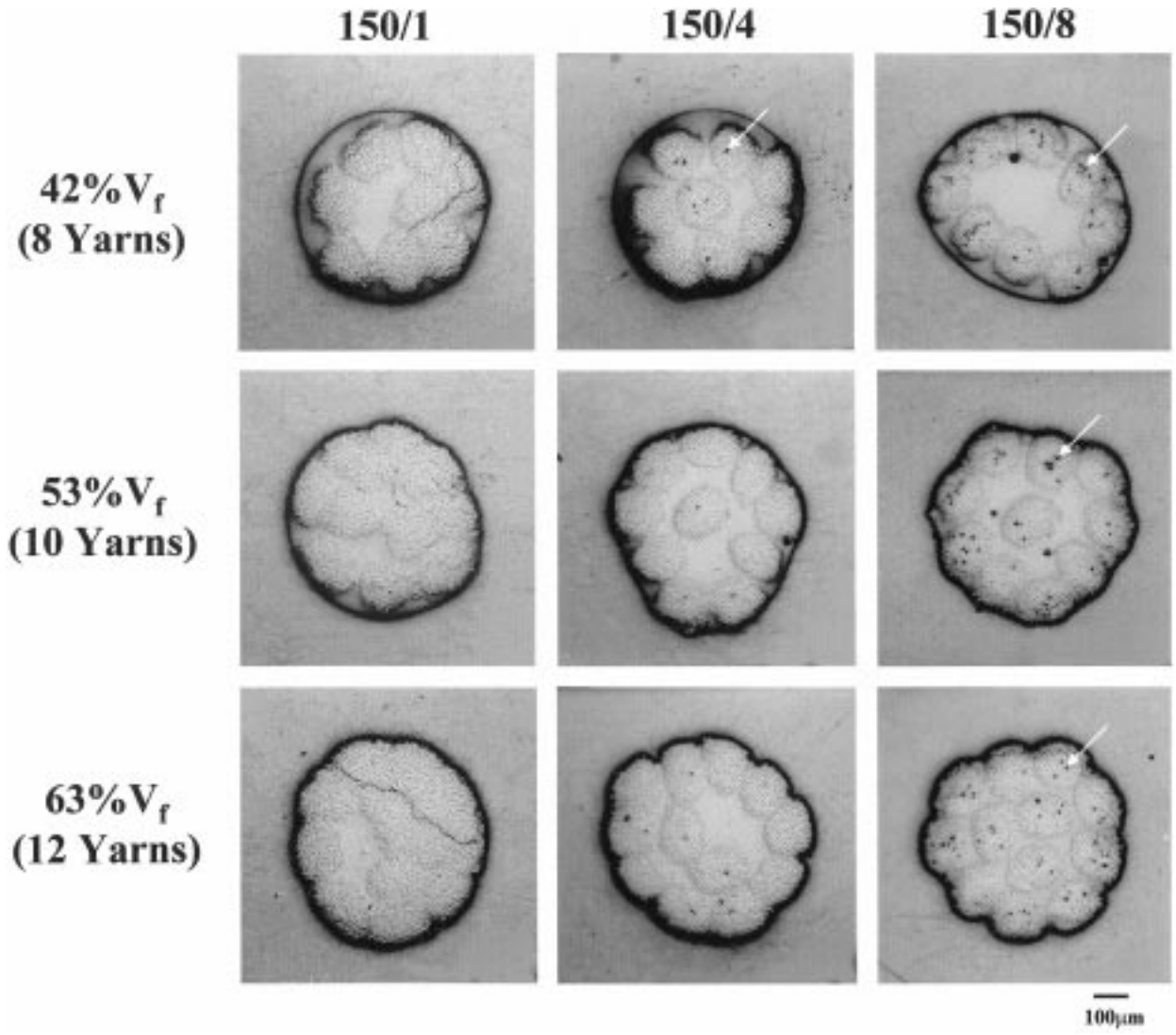

Figure 2 Photomicrographs of round, S2-glass® reinforced profiles at three loading levels: 42, 53 and 63%V_f or 8, 10 and 12 yarns. The numbers at the top of the columns indicate CG150 yarns of 1, 4 and 8 TPI, respectively. Arrows identify intra-yarn voids.

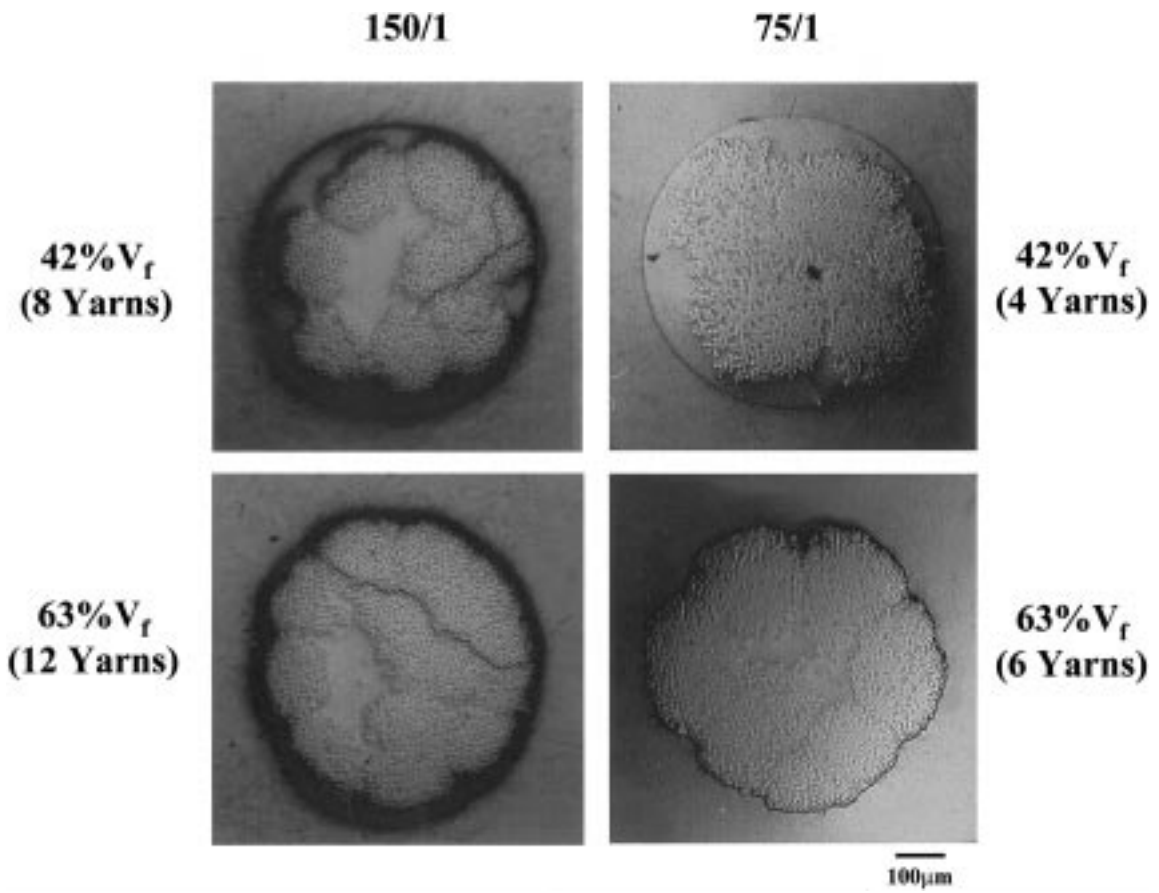

Figure 3 Photomicrographs of round, S2-glass® reinforced profiles of two deniers at two loading levels. The numbers at the top of the columns denote deniers of 150 and 75 for 1 TPI yarns. The numbers to the left and right of the rows denote the loading levels in terms of $\%V_f$s and the numbers of reinforcement yarns (each row shows equivalent $\%V_f$s even though the number of yarns differ).

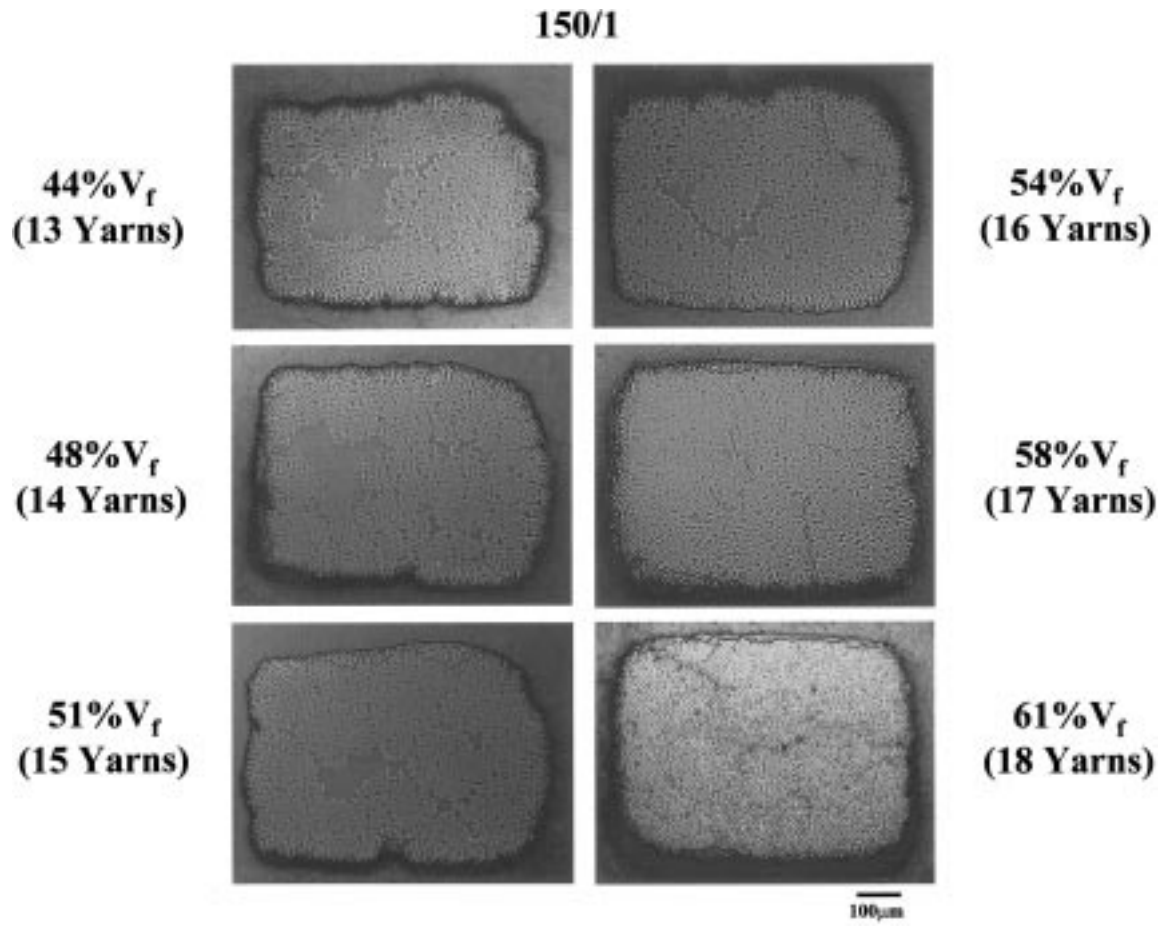

Figure 4 Photomicrographs of rectangular, S2 CG150/1 TPI-glass® reinforced profiles at six levels of reinforcement: 44, 48, 51, 54, 58 and 61$\%V_f$ or 13, 14, 15, 16, 17 and 18 yarns.

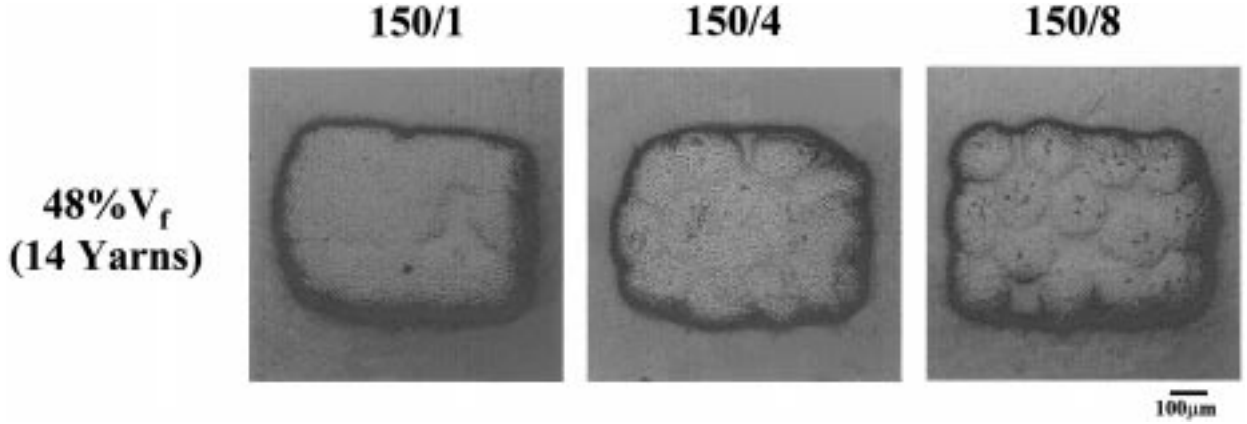

Figure 5 Photomicrographs of various rectangular, S2-glass® reinforced profiles at 48%V_f. The numbers at the top indicate CG150 yarns of 1, 4 and 8TPI, respectively.

profiles was less than 5% of mean values for Es and generally less than 10% for FSs. When mean Es for round and rectangular profiles were plotted (Figs 6 and 7), a positive correlation with theoretical values predicted by the rule of mixtures for fiber-reinforced composites [20], was generally observed (Figs 6 and 7, dotted line) Statistical analyzes (Figs 6 and 7 right side) revealed that significant changes occurred when %V_f, denier, and TPI were altered (Figs 6 and 7, right side).

4. Discussion

4.1. Morphology (round)

The type of reinforcement fiber greatly influenced the morphology as well as the loading characteristics of these round, unidirectional, fiber-reinforced composites. As the TPI of the yarn was increased from 1 to 8, the yarn tended to retain its intra-yarn cohesion following the spreading procedure, which led to more isolated and peripherally placed yarns in the finished profile (Fig. 2, row 1). This characteristic also had the negative effect of inhibiting ideal fiber separation during the spreading procedure, leading to incomplete resin coating and intra-yarn voids (Fig. 2, arrows). As the %V_fs of 4 and 8 TPI yarns were increased, the external surfaces of the samples became increasingly more convoluted, assuming the characteristic cross-sectional outline of a multistranded orthodontic archwire (Fig. 2, columns 2 and 3).

With the profile dimensions utilized, nine yarns $(48\%V_f)$ could be placed to fill the periphery completely. Within the CG150/1 TPI group (Fig. 2, column 1), the yarns loaded centrally until sufficient numbers of yarns were present to allow external surface tension to draw them toward the periphery. The CG150/1 TPI group attained a peripheral loading of nine yarns only after 12 yarns were incorporated $(63\%V_f)$. Three yarns were needed in the central core to allow complete peripheral loading. Within the CG150/4TPI group (Fig. 2, column 2), the yarns also loaded centrally until a sufficient number was present to allow complete peripheral loading of nine yarns after 10 yarns were incorporated $(53\%V_f)$. One yarn was placed centrally. An unusual observation was noted within the CG150/4 TPI group in that at a loading level of 12 yarns $(63\%V_f)$, a tenth yarn was forced into the periphery. This occasional finding

TABLE II Summary of flexural properties for round composite profiles

Yarn type	Loading (%V_f)	Loading (#yarns)	Elastic modulus, E (GPa)*	Flexural strength, FS (GPa)*
CG75/1 TPI	32	3	21.3 ± 2.1 (9)	1.02 ± 0.12 (12)
	42	4	29.4 ± 5.3 (18)	1.12 ± 0.11 (10)
	53	5	43.2 ± 5.5 (13)	1.36 ± 0.17 (13)
	63	6	46.0 ± 1.8 (4)	1.35 ± 0.10 (7)
CG150/1 TPI	42	8	33.7 ± 5.7 (17)	1.11 ± 0.11 (10)
	48	9	34.7 ± 3.9 (11)	1.18 ± 0.11 (9)
	53	10	37.8 ± 1.3 (3)	1.18 ± 0.13 (11)
	63	12	44.5 ± 3.1 (7)	1.34 ± 0.14 (10)
	74	14	53.6 ± 2.0 (4)	1.23 ± 0.09 (7)
CG150/4 TPI	43	8	29.5 ± 3.0 (10)	1.08 ± 0.08 (7)
	48	9	39.5 ± 2.2 (6)	1.09 ± 0.13 (12)
	53	10	44.9 ± 3.8 (8)	1.26 ± 0.15 (12)
	64	12	52.5 ± 3.1 (6)	1.23 ± 0.08 (7)
	74	14	52.4 ± 3.3 (6)	1.25 ± 0.12 (10)
CG150/8 TPI	43	8	29.7 ± 2.6 (9)	1.07 ± 0.06 (6)
	54	10	40.8 ± 2.8 (7)	0.98 ± 0.04 (4)
	65	12	39.5 ± 1.4 (4)	1.01 ± 0.03 (3)

*Mean ± one standard deviation (s.d.) for five specimens tested. The number in parentheses represents the precision as a per cent = 100(s.d./mean).

TABLE III Summary of flexural properties for rectangular composite profiles

Yarn type	Loading (%V_f)	Loading (#yarns)	Elastic modulus, E (GPa)*	Flexural strength, FS (GPa)*
CG75/1 TPI	41	6	28.9 ± 0.4 (1)	0.91 ± 0.08 (9)
	48	7	34.0 ± 1.1 (3)	1.05 ± 0.05 (5)
	54	8	39.3 ± 1.2 (3)	1.25 ± 0.07 (6)
	61	9	45.7 ± 0.8 (2)	1.40 ± 0.05 (4)
CG150/1 TPI	41	12	19.6 ± 0.3 (2)	0.78 ± 0.06 (8)
	48	14	32.7 ± 0.6 (2)	0.98 ± 0.11 (11)
	54	16	36.7 ± 0.3 (1)	1.07 ± 0.11 (10)
	61	18	38.6 ± 1.8 (5)	1.17 ± 0.06 (5)
CG150/4 TPI	48	14	30.2 ± 1.4 (5)	1.04 ± 0.07 (7)
CG150/8 TPI	48	14	32.4 ± 0.3 (1)	0.84 ± 0.06 (7)

*Mean ± one standard deviation (s.d.) for five specimens tested. The number in parentheses represents the precision as a per cent = 100(s.d./mean).

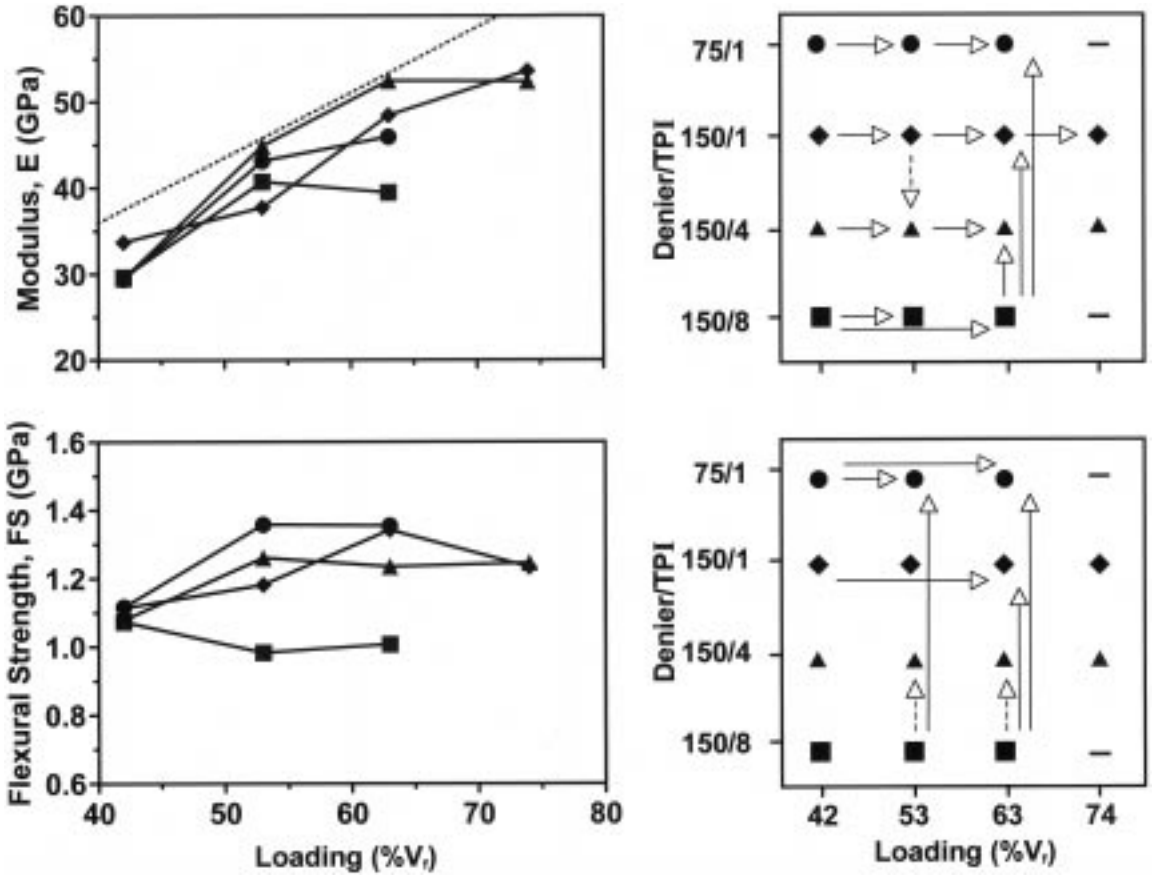

Figure 6 Plots of mean values and statistical comparisons of flexural properties for round profiles of CG75/1 TPI (●) and CG150 yarns at 1 TPI (◆), 4 TPI (▲) and 8 TPI (■) at various levels of reinforcement. The dotted line represents theoretical values according to the rule of mixtures [20]. The open arrows (—▷) denote highly significant comparisons at $p < 0.001$; whereas, the dotted arrows (---▷) denote significant comparisons at $p < 0.05$. The arrow points to the higher mean value.

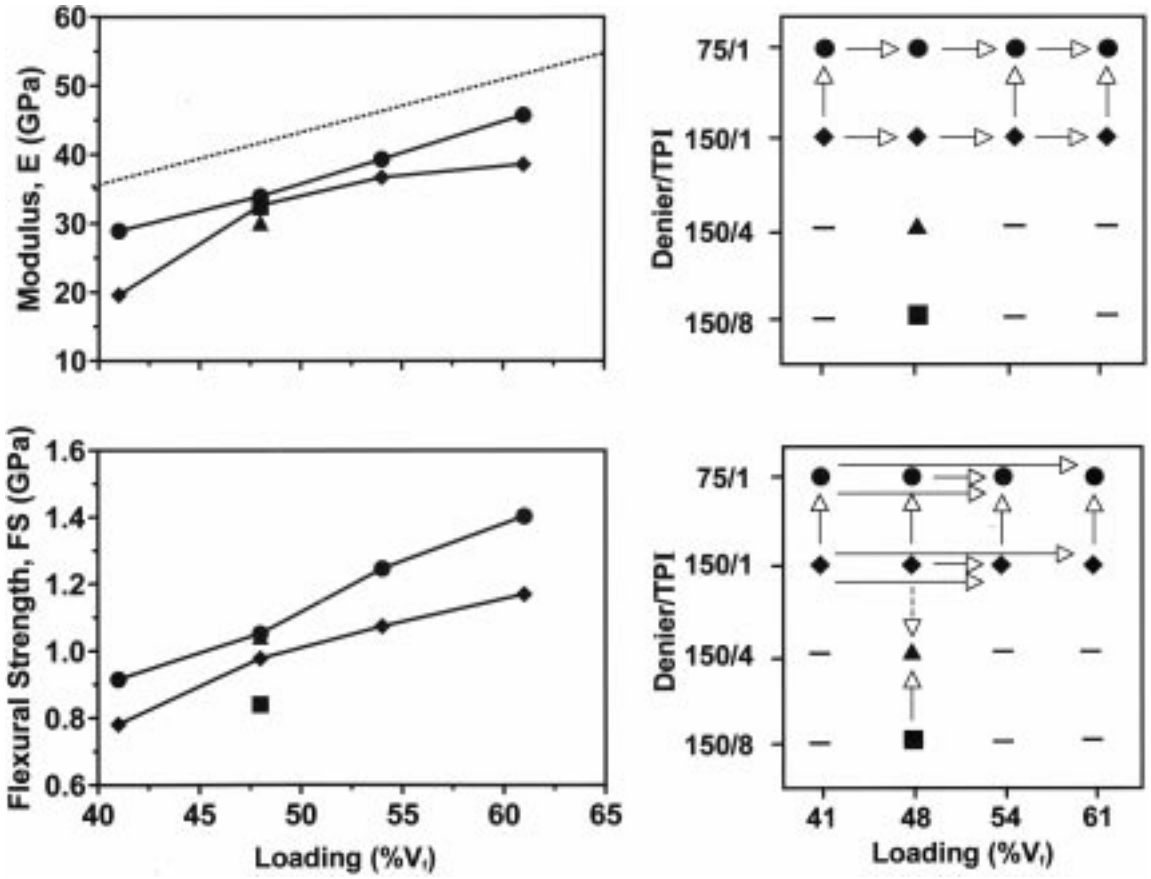

Figure 7 Plots of mean values and statistical comparisons of flexural properties for rectangular profiles of CG75 and CG150 yarns of 1 TPI (● and ◆, respectively) at various levels of reinforcement and of CG150 yarns of 4 TPI (▲) and 8 TPI (■) at 48%V_f. The dotted line [20], open arrows (—▷) and dotted arrows (---▷) have the same connotations as in Fig. 6.

appeared to be a direct result of the greater intra-yarn cohesion leading to a tighter packing of yarns within the profile. Within the CG150/8 TPI group (Fig. 2, column 3), the yarns loaded peripherally even before the ideal number was present for complete peripheral loading. Peripheral loading occurred with eight yarns ($42\%V_f$), prior to the presence of the geometrically optimal level of nine yarns ($48\%V_f$).

When the denier of the reinforcement was varied in round profiles, differing morphological characteristics were observed. As with previous 1 TPI yarns, loading began centrally and progressed peripherally until the profile was completely filled. At lower loading levels the circular geometry was better in both groups (Fig. 3, row 1); at high loading levels the geometry of the CG75/1 TPI group was negatively affected by an increase in yarn size (Fig. 3, row 2). Based upon these observations, increasing the denier of the yarn had some beneficial effects when the loading was low; however, the large denier yarns apparently influenced more the morphology of these composites at high $\%V_f$.

4.2. Morphology (Rectangular)

Evaluation of rectangular samples revealed that when CG150/1 TPI yarns were used for reinforcement, the yarns initially loaded more peripherally leaving a matrix-rich zone in the center of the profile. As additional yarns were added the matrix-rich zone decreased in area, although yarns were still being forced further to the periphery (Fig. 4). ''Filling-out'' of the die and the resultant optimal rectangular profile were not observed until 17 yarns were incorporated ($58\%V_f$).

As seen in the loading characteristics of round profiles, the incorporation of increased twists per inch enhanced yarn isolation, increased peripheral loading at lower loading levels, and increased intra-yarn voids. Optimal rectangular morphology was observed at 14 yarns ($48\%V_f$) when CG150/4 TPI and CG150/8 TPI yarns were used for reinforcement (Fig. 5). Moreover, as in round profiles, a convoluted external surface was evident. Based upon these observations, reinforcement of rectangular composite profiles with yarns incorporating more twists per inch apparently facilitates the attainment of the ideal rectangular morphology at lower $\%V_f$. This is most likely a result of the greater tendency of the twisted fibers to load peripherally, filling-out the die.

Although not shown, a comparative evaluation of the effects of increased denier (CG75 versus CG150) at 1 TPI revealed no appreciable differences in the morphology of rectangular profiles.

4.3. Flexural properties

In the study of anisotropic composite materials, we expect that at least E would follow the ''rule of mixtures'' [20]. To evaluate this assumption, the theoretical values were calculated and compared with the experimental values observed in this study (Figs 6 and 7, dotted lines versus data). When 1 TPI fibers were utilized, the E of the round and rectangular profiles generally increased as a function of fiber content in agreement with the rule of mixtures, albeit offset somewhat by the inefficiency caused by the less than perfect adhesion. When 4 and 8 TPI fibers were utilized, E reached a maximum value after which additional loading was ineffective.

The FSs reached an optimal level, after which additional loading was not beneficial. This optimal level seemed dependent upon the denier of the yarn utilized for reinforcement, with the highest FSs being reached when the CG75 yarn was used. This optimal level was also dependent upon the TPI of the reinforcement yarn, with optimal FSs being reached at successively lower $\%V_f$s as the TPIs increased. These optimal FSs occurred coincidently with optimal peripheral loadings (Fig. 2).

For the CG150/1 TPI *round profiles* of the group, the Es continued to rise as a function of fiber content to a maximum value of $74\%V_f$ (14 yarns) (Fig. 6, upper left). The FS reached the highest level at $63\%V_f$ (12 yarns) (Fig. 6, lower left), which corresponded to the level at which optimal peripheral loading occurred (Fig. 2, column 1). Additional loading did not increase the strength once the periphery of the profile was filled (Fig. 6, lower right). The E and FS were not significantly altered for the same $\%V_f$, when the denier of the reinforcement fiber was doubled (Fig. 6, right).

In the CG150/4 TPI group, the E continued to rise as a function of fiber content to the level of $63\%V_f$ (12 yarns) (Fig. 6, upper left), after which no significant difference was noted (Fig. 6, upper right). The FS reached its highest level at $53\%V_f$ (10 yarns) (Fig. 6, lower left), which corresponded to the first loading level after which optimal peripheral loading occurred (Fig. 2, column 2). Although the maximum strength occurred at this $\%V_f$, no statistically significant difference was observed at any $\%V_f$ (Fig. 6, lower right).

In the CG150/8 TPI group, the E increased to a maximum value at $53\%V_f$ (10 yarns) (Fig. 6, upper left), which was a significant change from the E at $42\%V_f$ (8 yarns). A further increase in $\%V_f$ to $63\%V_f$ (12 yarns) resulted in no significant change (Fig. 6, upper right). The FS reached its highest level by $42\%V_f$ (8 yarns) (Fig. 6, lower left), which corresponded to the first level observed to have all reinforcement yarns peripherally placed (Fig. 2, column 3). The maximum FS occurred at $42\%V_f$ but was not significantly different from the values observed at other levels (Fig. 6, lower right).

Evaluation of *rectangular profiles* revealed that when 1 TPI fibers were utilized, both E and FS increased as a function of fiber content at all loading levels (Fig. 7, left). Comparisons between the two 1 TPI groups revealed that when the denier was doubled (CG75 versus CG150), an increase in E occurred, whose difference was highly significant at all loading levels except $48\%V_f$ (Fig. 7, upper right). Comparison of FSs revealed an increase at all loading levels (Fig. 7, lower right).

Evaluation of $48\%V_f$ samples as a function of TPI revealed that an increase in TPI resulted in no significant change in E (Fig. 7, upper right). However, an increase in TPI resulted in a decrease in the FS of the CG150/8 TPI group that was highly significant (Fig. 7, lower right). This decrease in FS appears to be a direct result of the decreased efficiency of fiber-matrix interfacial bonds as

TABLE IV Comparison of flexural properties for conventional orthodontic materials and pultruded composites

Material	Reference		Elastic modulus, E (GPa)*	Flexural strength, FS (GPa)*
	E	FS		
Conventional Orthodontic Materials				
Stainless steel	[23]	[23]	181–206	2.10–2.85
Cobalt-chromium	[24]	[24]	196	2.34
Martensitic nickel titanium	[21]	[21]	33.4–44.4	1.55–1.93
Beta-titanium	[21]	[21]	72.4	1.31–1.50
Thermally-pultruded Composites				
E glass reinforced				
70%V_f-unidirectional	[2]	[2]	41.4	0.69
S2 glass® reinforced				
[a]42%V_f-unidirectional	[22]	[22]	17.9	0.43
[b]43%V_f-unidirectional	[3]	[3]	19.7	0.55
[c]45%V_f-unidirectional	[3]	[3]	21.1	0.58
Photo-pultruded Composites				
Quartz reinforced				
[d]38%V_f-unidirectional	[9]	[9]	25	1.4
[d]70%V_f-unidirectional	[9]	[9]	45	2.1
[d]75%V_f-unidirectional	[13]	[13]	45.2	0.94
E glass Reinforced				
[d]70%V_f-unidirectional	[13]	[13]	38.8	1.14
S2 glass® reinforced				
[d]42%V_f-unidirectional	Table II		29.4	1.12
[d]46%V_f-unidirectional	[13]	[13]	35.9	1.20
[c]57%V_f-unidirectional	[14]	[14]	45.1–47.2	1.15–1.72
[d]61%V_f-unidirectional	Table III		45.7	1.40
[d]70%V_f-unidirectional	[13]	[13]	47.7	1.29
d74%V_f-unidirectional	Table II		53.6	1.23
[d]79%V_f-unidirectional	[13]	[13]	56.4	0.77

[a]Polycarbonate polymeric matrix.
[b]Poly(ethylene terephthalate glycol) polymeric matrix.
[c]Poly(1,4-cyclohexylene dimethylene terephthalate glycol) polymeric matrix.
[d]61%$_{wt}$ BIS-GMA and 39%$_{wt}$ TEGDMA (formulation used in current study).
[c]60%$_{wt}$ BIS-GMA and 40%$_{wt}$ methylmethacrylate.

evidenced by the increased number of intra-yarn voids (Figs 2 and 5).

4.4. In perspective

When loading was optimized according to $\%V_f$, denier, and TPI, the maximum mean Es and FSs equaled 53.6 ± 2.0 and 1.36 ± 0.17 GPa for round profiles and equaled 45.7 ± 0.8 and 1.40 ± 0.05 GPa for rectangular profiles, respectively (Tables II and III). Comparison of these E and FS values with other traditional and experimental materials (Table IV) [2, 3, 9, 13, 14, 21–24] revealed that these materials could be engineered to exhibit a range of Es while demonstrating superior FSs than comparable reinforced plastics. When compared to currently available orthodontic archwires, moreover, these Es were midway between martensitic NiTi (44.4 GPa for round and 33.4 GPa for rectangular) and beta-titanium (72.4 GPa), that is, about one-quarter that of stainless steel (181–206 GPa) [21, 23]. Comparison of FS values placed this composite material in the range of published values for beta-titanium wires (1.3–1.5 GPa) [21].

The round profiles having the highest mean E value (53.6 ± 2.0 GPa) were fabricated with CG150/1 TPI fibers at $74\%V_f$. When the TPI was increased using CG150/4 TPI fibers, E equaled 52.5 ± 3.1 GPa at only $64\%V_f$ with identical FSs of 1.23 ± 0.08 GPa (Table II). Consequently, the incorporation of 4 TPI in the reinforcement fibers may be beneficial in round composites when higher Es are desired for a given $\%V_f$ (Fig. 6) or when a higher degree of peripheral loading of yarns is desired (Fig. 2).

The highest FSs in round and rectangular profiles were observed when composites were fabricated with CG75/1 TPI fibers (Figs 6 and 7). When compared to CG150/1 TPI fibers, the CG75/1 TPI fibers produced a statistically significant difference in rectangular profiles, although the change noted for round profiles was not significant. Apparently increasing the denier of the reinforcing yarns improved the FS values, which are dependent upon many factors: (1) the individual strengths of the fibers; (2) the $\%V_f$s; (3) the orientation of the fibers; (4) damage to the fibers during manufacture; and (5) the efficiencies of the fiber-matrix interfacial bonds. In this study most of these factors were maintained, while the denier was altered. Since the number of intra-yarn voids were comparable in the CG75/1 TPI and CG150/1 TPI groups (Fig. 3), the efficiency of the fiber-matrix interfacial bond is not a major contributor to the increase in FS. On the other hand, increasing the number of glass fibers per yarn increases the likelihood of fiber uniformity by decreasing the number of independently oriented yarns within the profile. This enhancement of fiber alignment results in a more uniform transfer of load to the fiber resulting in an increased FS. Also, due to the increased size of the CG75 yarns, relatively speaking about 30% fewer fibers are exposed at the circumference of these yarns as compared to the equivalent $\%V_f$ of CG150 yarns. In absolute terms then, when compared at $63\%V_f$, about 200 fewer fibers are immediately susceptible to damage during handling in a 0.022 in (0.56 mm) round wire prior to photo-pultrusion (Appendix).

5. Conclusions

The manufacture of continuous, small profile, rectangular composite profiles is possible utilizing this novel photo-pultrusion process. The incorporation of increased twists per inch (TPI) within the reinforcement yarns enhances yarn isolation (increases the matrix-rich zones between yarns), increases peripheral loading, and provides more ideal morphology at lower loading levels ($\%V_f$s), but inhibits ideal polymer coverage during manufacture and leads to voids.

The incorporation of 4 TPI in the reinforcement fibers may be beneficial, when a higher modulus (E) is desired for a given $\%V_f$ but this benefit appears dependent on the $\%V_f$ selected. The incorporation of 8 TPI yarns does not enhance flexural strength (FS) at any $\%V_f$.

The Es increase as a function of loading in accordance with the rule of mixtures when 1 TPI fibers are utilized. When 4 TPI and 8 TPI fibers are utilized for reinforcement, E reaches an optimal level, after which additional loading is ineffective. These optimal E s are reached at lower $\%V_f$ levels as the TPI is increased.

For FSs, an optimal $\%V_f$ is reached in all materials

after which additional loading is ineffective. In round profiles utilizing 1 TPI and 4 TPI fibers, the optimal FS coincided with optimal peripheral loading.

When the denier is increased (by increasing the number of filaments per yarn), the FSs of round and rectangular profiles increase.

Appendix

The difference between the diameters of the S2-glass® yarns [$D_{75} = 0.011$ in. (0.27 mm) for the CG75 yarn versus $D_{150} = 0.008$ in. (0.20 mm) for the CG150 yarn] is due to a difference in the number. N, of constituent glass filaments per yarn (408 for CG75 yarn versus 204 for CG150 yarn) (Fig. A1), according to the equation,

$$N_{75} = 2 \times N_{150} \quad \text{(A1)}$$

When equal numbers of filaments are compared between the yarns, their diametric difference results in a decreased overall circumference, C, of the one CG75 yarn as compared to the two CG150 yarns according to the equations,

$$C_{75} = \pi\, D_{75} \quad \text{(A2)}$$

$$= \pi(0.011\,\text{in. or } 0.28\,\text{mm})$$

$$= 0.035\,\text{in. or } 0.88\,\text{mm}$$

and

$$C_{150} = 2\pi\, D_{150}$$

$$= 2\pi(0.008\,\text{in. or } 0.20\,\text{mm})$$

$$= 0.05\text{in. or } 1.28\text{mm.} \quad \text{(A3)}$$

Therefore, from Equations A2 and A3,

$$C_{75} = 0.7\, C_{150} \quad \text{(A4)}$$

This decrease in the overall circumference of the CG75 yarn results in a 30% decrease in the number of exposed filaments that are susceptible to damage during handling and the pultrusion processing.

The actual number of these 0.000354 in. (9 μm) diameter exposed filaments, N^*, in each yarn can be theoretically determined for the CG75 (N^*_{75}) yarn and the CG150 (N^*_{150}) yarns according to the equations,

$$N^*_{75} = \mathrm{C}_{75}/(0.000345\,\text{in. or } 9\,\mu\text{m}) \quad \text{(A5)}$$

and

$$N^*_{150} = \mathrm{C}_{150}/(0.000354\,\text{in. or } 9\,\mu\text{m}) \quad \text{(A6)}$$

Substituting the outcomes of Equations A2 and A3 into Equations A5 and A6 respectively, yields 98 exposed

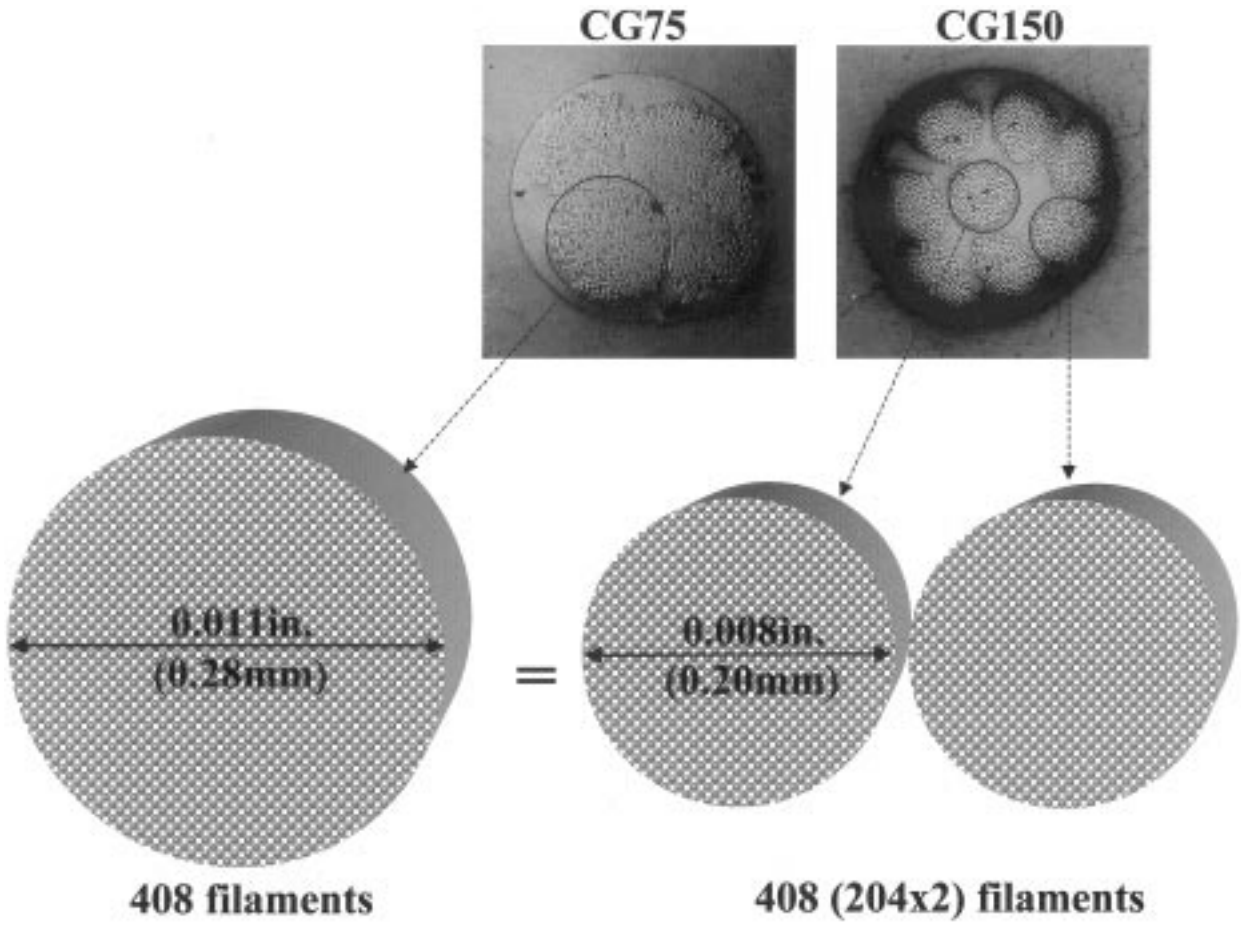

Figure A1 Photomicrographs and schematic representation of the numbers of constituent filaments and diametric differences between the CG75 and CG150 yarns.

filaments for one CG75 yarn and 140 (70 per yarn) exposed filaments for two CG150 yarns.

In absolute terms, the 63% V_f, 0.022 in. (0.56mm) diameter profiles incorporate either 6, CG75 yarns or 12, CG150 yarns with equal numbers of filaments (see Fig. A1 in which 4 and 8 yarns are used to demonstrate yarn distribution). Assuming an ideal heterogeneous distribution of filaments (100% around the circumference), there would be 588 total exposed filaments in the 63% V_f, 0.022 in. (0.56mm) diameter, CG75 profile (98×6) and 840 total exposed filaments in the CG150 profile (70×12), for a total of 252 fewer exposed filaments. Assuming a more realistic homogeneous distribution of filaments (63% around the circumference), there would be 370 exposed filaments in the CG75 profile (0.63×588) and 529 exposed filaments in the CG150 profile (0.63×840), for a total of 159 fewer exposed filaments. An average of these two values (since the truest number is, most likely, somewhere in between these two values) reveals that approximately 200 fewer fibers are exposed in the 63% V_f, 0.022 in. (0.56mm) diameter composite when CG75 yarns are used in comparison to CG150 yarns.

6. Acknowledgments

The authors would like to thank Mr John Q. Whitley for artwork, the UNC-CH Department of Orthodontics for financial support, and Owens Corning Corp. and Atkins-Pearce Corp. for contributing the S2-glass® yarn materials.

Notes

1. Denier, a measure of fiber size, is defined as the weight in grams of a 9000-meter length of fiber [17]. The manufacturer reports a converted yarn size by way of a coding system with the first number representing 1/100th the total approximate bare glass yardage in a pound of strand. The yardage per pound is then divided into a constant (4.5×10^6) to calculate a denier equivalent.

References

1. M. DAVIDSON, *Adv. Mater. & Prod.* **146** (1994) 70.
2. T. J. REINHART and L. L. CLEMENTS, in ''Engineered Materials Handbook, Vol. 1; Composites'' (ASM International 1987) p. 28.
3. A. J. GOLDBERG and C. J. BURSTONE, *Dent. Mater.* **8** (1992) 197.
4. A. C. KARMAKER, A. T. DIBENEDETTO and A. J. GOLDBERG, *J. Biomater. Appl.* **11** (1997) 318.
5. J. JANCAR, A. T. DIBENEDETTO and A. J. GOLDBERG, *J. Mater. Sci.: Mater. Med.* **4** (1993) 562.
6. J. JANCAR, A. T. DIBENEDETTO, Y. HADZIINIKOLAU, A. J. GOLDBERG and A. DIANSELMO, *ibid.* **5** (1994) 214.
7. J. JANCAR and A. T. DIBENEDETTO, *ibid.* **4** (1993) 555.
8. R. P. KUSY and K. C. KENNEDY, U.S. Patent No. 5 869 178 (1999).
9. K. C. KENNEDY and R. P. KUSY, *J. Vinyl Additive Technol.* **1** (1995) 182.
10. V. NARAYANAN and A. B. SCRANTON, *Trends in Polymer Sci.* **5** (1997) 415.
11. K. C. KENNEDY, T. CHEN and R. P. KUSY, *J. Mater. Sci.: Mater. Med.* **9** (1998) 243.
12. *Idem.*, *ibid.* **9** (1998) 651.
13. *Idem.* in ''Advanced Composites X. Proceedings of the 10th Annual ASM/ESD Advanced Composites Conference & Exposition'', Dearborn, MI, Nov. 7–10, 1994 (ASM International, Materials Park, OH, 1994) p. 191.
14. K. C. KENNEDY and R. P. KUSY, *J. Biomed. Mater. Res.* **41** (1998) 549.
15. C. J. BURSTONE, *Am. J. Orthod.* **80** (1981) 1.
16. R. P. KUSY, *The Angle Orthodontist* **67** (1997) 197.
17. R. A. FLINN and P. K. TROJAN, ''Engineering Materials and Their Applications'', 3rd edn (Houghton Mifflin Company, Boston, 1986) p. 447.
18. O. W. ESHBACH and M. SOUDERS, ''Handbook of Engineering Fundamentals'' 3rd edn (John Wiley and Sons, New York, NY, 1975) pp. 513 and 518.
19. R. P. KUSY and L. E. STEVENS, *The Angle Orthodontist* **57** (1987) 18.
20. J. F. SHACKELFORD, ''Introduction to Materials Science for Engineers'' 2nd edn (Macmillan Publishing Co., New York, NY, 1988) p. 473.
21. R. P. KUSY and A. M. STUSH, *Dent. Mater.* **3** (1987) 207.
22. A. J. GOLDBERG, C. J. BURSTONE, I. HADJINIKOLAOU and J. JANCAR, *J. Biomed. Mater. Res.* **28** (1994) 167.
23. R. P. KUSY, G. J. DILLEY and J. Q. WHITLEY, *Clinical Mater.* **3** (1988) 41.
24. Elgiloy® and Tru-Chrome® Stainless Steel Orthodontic Treatment Wires, promotional literature of Rocky Mountain Orthodontics (1977) p. 5.

Received 30 March 1999
and accepted 24 August 1999